Orchestrating Distributed Assets to Expand Resilience During Rolling Outages

Shiva Poudel, Monish Mukherjee, Min Gyung Yu, and Akshay Kumar Jain
Pacific Northwest National Laboratory, Richland, WA, USA
Richland, WA 99354
{shiva.poudel, monish.mukherjee, mingyung.yu, akshaykumar.jain}@pnnl.gov

***Abstract*—This paper presents a two-stage outage management approach that enhances distribution system resilience by leveraging distributed assets to share limited power across all customers during scarcity conditions. In the proposed framework, resource scheduling and rolling outage optimization are jointly utilized to allocate available capacity in a manner that minimizes service disruptions and ensures a more balanced distribution of power across all customers, including those without generation or storage assets. The approach is demonstrated using a taxonomy feeder model and weather data from the 2021 winter storm Uri. Simulation results show that coordinated asset operation can significantly reduce outage duration and improve overall service restoration. A comparison with traditional unit resilience—where customers rely solely on their own assets—illustrates the distinct system-level value of shared resilience, achieved through coordinated management. These results highlight the opportunity for Distribution System Operators (DSOs) to design mechanisms and incentive structures that enable and sustain shared resilience at scale.**

***Index Terms*—Advanced metering infrastructure, extreme weather events, grid resilience, unit resilience, and load management**

I. Introduction

The increasing frequency of extreme weather events is causing significant disruptions to power systems worldwide, with outages becoming more common due to snowstorms, hurricanes, and heat waves. Temperature-related events, in particular, exacerbate challenges for utilities as they drive demand to extreme levels while often creating generation scarcity and stressing infrastructure limits [1]. During extreme weather events, such as the 2021 winter storm in Texas and the 2020 heatwave in California, the electric grid faced severe stress; frigid temperatures and soaring heat caused unprecedented spikes in heating and cooling demand, while generation and transmission systems were simultaneously strained, resulting in widespread outages and rolling blackouts that affected millions [2].

Extreme weather events make it more challenging for utilities to maintain the balance between electricity supply and demand in order to minimize outage risks. Outage management during scarcity can be handled via different rolling outage mechanisms based on automation technologies [3]. Utilities are increasingly investigating the potential of the customer-sited distributed assets (DAs) to enhance grid resilience, affordability, and reliability; for example, Vermont's Green Mountain Power is proposing to install battery storage systems in remote homes as part of a program to reduce outages and lower costs [4], while in the Northwest, behind-the-meter generation-battery systems are being used to help manage peak demand, illustrating how DAs can influence customer participation and operational outcomes on the grid [5].

During emergency conditions, these resources can keep customers powered for certain hours, maintaining not only indoor comfort during extreme temperature events but also supporting essential customer functions—an effect we refer to as unit resilience [6], [7]. This localized benefit improves resilience only for the specific loads served by the on-site generation or storage. Because these resources operate strictly behind the meter in the unit-resiliency case and are not exported back to the grid beyond normal operations, they do not meaningfully reduce the extent of outages or enhance resilience at the system level. In contrast, shared resilience utilizes DAs collectively, often through advanced coordination, aggregation, and integration with grid control systems, to support broader distribution system restoration and load management, thereby reducing the scope and duration of outages for many customers. Leveraging DAs for shared resilience, however, necessitates new outage management strategies and distribution system controls that can effectively orchestrate these assets [8].

In this paper, we propose a novel approach to orchestrating DAs and coordinating switching schemes under the shared resilience concept, examining the trade-offs and synergies with unit-level resilience. This approach aims to maintain sufficient individual customer comfort while enhancing system-wide resilience in response to increasingly severe temperature-driven events. The specific contributions of this paper are twofold:

1) Develop a two-stage optimization framework for the orchestration of DAs and switching scheme design in rolling outage management. The first stage schedules Battery Energy Storage Systems (BESS) based on forecast load and generation, while the second stage determines rolling outage actions considering effective availability influenced by the schedules of DAs.
2) Compare the proposed approach with the concept of unit resilience to quantify how outage management that leverages DAs can extend service support to a broader set of customers during scarcity events.

This material is based on work funded by the U.S. Department of Energy, Office of Electricity, Grid Controls and Communications Program.

979-8-3315-8138-1

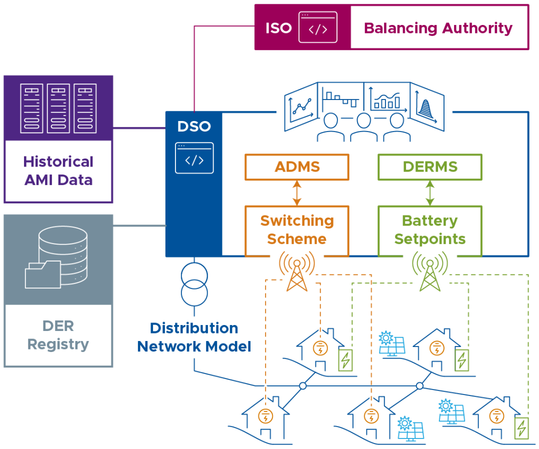

Fig. 1. AMI-based rolling outage including controls for distributed assets.

II. Methodology

To enhance distribution system resilience during emergency operating conditions, a two-stage outage management methodology is proposed, as illustrated in Fig. 1. In the first stage, the Distribution Energy Resource Management System (DERMS) schedules customer Battery Energy Storage Systems (BESS) by leveraging the forecast substation load and the load shedding request received from the Independent System Operator (ISO). Since the BESSs are reserved for emergency operation, their dispatch is excluded from the base substation load forecast. This stage determines optimal BESS setpoints that can partially offset the required load reduction and reduce the need for customer outages.

In the second stage, the Advanced Distribution Management System (ADMS) implements a rolling outage mechanism to determine which customers should remain energized or temporarily curtailed, considering both the ISO load shedding requirement and the BESS support scheduled in the first stage. The DSO executes this stage by integrating customer-level Advanced Metering Infrastructure (AMI) data to assess localized load and stress conditions. This mechanism allows the DSO to comply with ISO directives while dynamically leveraging the available flexibility of the DAs to minimize customer disruption. In this study, we simulate a scenario in which the DSO directly operates customer-owned assets to support other customers, recognizing that such actions would typically require compensation mechanisms. While incentive design is outside the scope of this paper, this paper aims to demonstrate the value of shared resilience and can inform future efforts to develop appropriate incentives.

The mathematical formulations and optimization strategies corresponding to these two stages are presented in the following subsections.

A. DER-Assisted Rolling Outage

1) BESS Scheduling Problem: The objective function in (1) minimizes the total squared deviation of substation power flow sub_t from its mean value $\bar{y}$ across the optimization horizon T. This formulation penalizes significant hour-to-hour variations in power exchange between the feeder and the upstream network. By minimizing the variance of sub_t, the objective promotes a more balanced distribution of grid stress or scarcity across time, ensuring that no particular period experiences disproportionate loading.

TABLE I
NOTATION AND VARIABLE DESCRIPTIONS.

Symbol	Description
T	Number of time steps (hours).
N_b	Number of customers with batteries.
N_s	Number of customers with on-site generation.
P_t^{forecast}	Forecasted substation baseline power at time t.
$P_{i,t}^{\text{gen}}$	Forecasted available on-site generation of i^{th} unit at time t.
P_i^{rated}	Rated charge/discharge capacity of battery i.
C_i	Energy capacity of battery i.
η_i	Charge/discharge efficiency of battery i.
$\mathrm{soc}_i^{\min}$	Minimum allowable state of charge (p.u.).
$\mathrm{soc}_i^{\text{init}}$	Initial state of charge (p.u.).
$\mathrm{soc}_{i,t}$	State of charge of battery i at time t (p.u.).
$p_{i,t}^c$	Charging power of battery i at time t (kW).
$p_{i,t}^d$	Discharging power of battery i at time t.
$\lambda_{i,t}^c$	Binary indicator for charging status.
$\lambda_{i,t}^d$	Binary indicator for discharging status.
sub_t	Net substation power flow at time t (kW).
$\bar{y}$	Mean substation power over the optimization horizon.

$$\min_{p_{i,t}^c,\, p_{i,t}^d,\, \lambda_{i,t}^c,\, \lambda_{i,t}^d,\, \mathrm{soc}_{i,t},\, \mathrm{sub}_t,\, \bar{y}} \sum_{t=1}^{T} (\mathrm{sub}_t - \bar{y})^2 \tag{1}$$

where,

$$\bar{y} = \frac{1}{T} \sum_{t=1}^{T} \mathrm{sub}_t \tag{2}$$

The substation power balance in (3) ensures that, at every time step t, the net substation flow sub_t equals the baseline substation forecast P_t^{forecast} adjusted by the aggregate power of all batteries.

$$\mathrm{sub}_t = P_t^{\text{forecast}} + \sum_{i=1}^{N_b} \left(p_{i,t}^c + p_{i,t}^d \right), \quad \forall t = 1, \ldots, T \tag{3}$$

This approach effectively distributes charging and discharging actions across time, leveraging local generation to flatten the substation load profile and eliminate peaks at certain times.

Constraint (4) limits the total charging power at each time step based on the available on-site generation forecast P_t^{gen}. This ensures that the cumulative battery charging across all units does not exceed the local generation available, promoting local utilization of on-site generation rather than importing power from the upstream grid.

$$\sum_{i=1}^{N_b} p_{i,t}^c \leq \sum_{i=1}^{N_s} P_{i,t}^{\text{gen}}, \quad \forall t \tag{4}$$

Equation (5) describes the individual operating limits for each battery i. The state of charge (SoC), $\mathrm{soc}_{i,t}$, must remain within its minimum permissible value $\mathrm{soc}_i^{\min}$ and its rated maximum $\mathrm{soc}_i^{\max}$. The power limits restrict the charging and discharging power to within the rated power capacity P_i^{rated}. These limits are modulated by the binary variables $\lambda_{i,t}^c$ and $\lambda_{i,t}^d$, which represent the operational status of battery i at time t. When $\lambda_{i,t}^c = 1$, the battery is in charging mode and can

979-8-3315-8138-1

charge up to its rated capacity, while when $\lambda_{i,t}^d = 1$, it is in discharging mode and can deliver power up to P_i^{rated}.

$$\begin{aligned} \text{soc}_i^{\min} \le \text{soc}_{i,t} \le \text{soc}_i^{\max}, \quad \forall t, \forall i \in N_b, \\ 0 \le p_{i,t}^c \le \lambda_{i,t}^c P_i^{\text{rated}}, \quad \forall t, \forall i \in N_b, \\ -\lambda_{i,t}^d P_i^{\text{rated}} \le p_{i,t}^d \le 0, \quad \forall t, \forall i \in N_b. \end{aligned} \tag{5}$$

The mutual exclusivity constraint in (6) ensures that a battery cannot charge and discharge simultaneously.

$$\lambda_{i,t}^c + \lambda_{i,t}^d \le 1, \quad \forall t, \forall i \in N_b \tag{6}$$

Similarly, the SoC dynamics defined in (7) model the temporal evolution of stored energy in each battery. The SoC is updated based on the previous SoC and the net effect of discharging and charging powers, adjusted by the round-trip efficiency η_i and the battery capacity C_i.

$$\text{soc}_{i,t} = \text{soc}_{i,t-1} + \frac{p_{i,t-1}^d}{\eta_i C_i} + \frac{p_{i,t-1}^c \eta_i}{C_i} \quad \forall t, \forall i \in N_b \tag{7}$$

2) Rolling Outage Optimization Formulation: During power scarcity events, the goal is to identify a subset of customers that can be energized while ensuring that total power consumption remains within the available power. To promote fairness across multiple scheduling intervals, each customer is assigned a *stress level* or *pickup factor* that increases with the duration of the outage and decreases when the customer is supplied. The optimization problem for a given scheduling interval is formulated as:

$$\min_{x_i} - \sum_{i=1}^{N} \alpha_i x_i \tag{8}$$

subject to:

$$\sum_{i=1}^{N} P_i x_i + \sum_{i=1}^{N_b} \left(p_{i,t}^c + p_{i,t}^d\right) \le P_{avail} + \sum_{i=1}^{N_s} P_{i,t}^{\text{gen}} \tag{9}$$

$$x_i = 1, \quad \forall i \in \mathcal{M}, \tag{10}$$

$$x_i \in \{0, 1\}, \quad \forall i = 1, \ldots, N. \tag{11}$$

where:

- $x_i = 1$ if customer i is supplied (turned *on*), and $x_i = 0$ if the customer is in outage (turned *off*);
- α_i is the *pickup factor* or *stress level* of customer i, which increases with accumulated outage time;
- P_i denotes the maximum power demand (kW) of customer i;
- P_{avail} is the available substation power limit under current scarcity conditions at a given time interval;
- $\mathcal{M}$ is the set of mandatory customers (e.g., critical loads) that must remain energized.

After solving (8)–(11), the model identifies two disjoint sets: (i) $\mathcal{S}_{\text{on}} = \{i \mid x_i = 1\}$, the customers who are supplied during this interval, and (ii) $\mathcal{S}_{\text{off}} = \{i \mid x_i = 0\}$, the customers that remain in outage.

The objective in (8) minimizes the negative weighted sum of customer stress factors α_i. This is equivalent to maximizing the total stress of the customers being turned on, meaning that customers with higher accumulated stress (i.e., those who have experienced longer or more frequent outages) are prioritized for power restoration.

Constraint (9) ensures that the total load from all customers selected to be turned on does not exceed the available substation power P_{sub}. Note that P_{sub} is a function of load shedding call received from ISO and DA scheduling obtained from stage 1. Constraint (10) enforces that customers in the mandatory set $\mathcal{M}$ (e.g., metered or critical infrastructure customers) remain energized at all times, reflecting operational policy requirements. Finally, (11) specifies that each decision variable x_i is binary, representing the on/off operational state of customer i.

Once the optimal set of customers to supply has been determined, the stress levels α_i are updated in a post-processing step to reflect the new system state. Customers that remain in outage accumulate stress, while those that were supplied experience stress relief. The update rule is expressed as:

$$\alpha_i^{(k+1)} = \begin{cases} w\,\alpha_i^{(k)}, & \text{if } i \in \mathcal{S}_{\text{off}}, \\ \dfrac{\alpha_i^{(k)}}{w}, & \text{if } i \in \mathcal{S}_{\text{on}}, \end{cases} \tag{12}$$

where $w > 1$ is a weighting factor controlling the rate of stress escalation and recovery. The iterative update in (12) ensures that customers who have been off for longer periods become more likely to be selected in subsequent optimization rounds. At the same time, those who were recently turned on are deprioritized temporarily. Over time, the dynamic interaction between the optimization problem and the evolving stress factors results in a fair rotation of supply across all customers, while respecting system-level power constraints.

B. Rolling Outage-Aware Unit Resilience (UR)

To provide a comparative benchmark to the proposed framework, a hybrid framework combining centralized rolling outage control and local customer-level resilience strategy is considered. In this approach, the system-level rolling outage optimization (as described in (8)) is used to determine the on/off supply status of each customer at every scheduling interval, but replacing the power limit constraint (9) with a version that excludes on-site generation and BESS contributions, as like $\sum_{i=1}^{N} P_i x_i \le P_{avail}$. This reflects a centralized rolling outage decision that considers only the available feeder/substation capacity, without accounting for customer-owned assets. Each customer (unit) will manage its own assets based on that supply status. At every decision interval:

- If customer i is selected as **supplied group** ($x_i = 1$), the customer remains connected to the grid. The local generation is first used to charge the local BESS if capacity is available. During this interval, the battery does not discharge, as the grid supply is available. When local generation exceeds the BESS capacity, the excess generated power is sent to the grid.
- If customer i is placed in the **outage group** ($x_i = 0$), the customer is completely isolated from the grid (meter

979-8-3315-8138-1

turned off). The local unit then relies solely on its own assets. The BESS can discharge to supply as much of the load as possible. Customers equipped with both on-site generation and BESS can generate and store energy for later use, thus maintaining the highest level of self-sufficiency. Customers with on-site generation can utilize power only during the daytime, while those with only BESS depend entirely on the stored energy available at the onset of the outage. Customers without both generation and BESS experience a complete service interruption when disconnected.

Each customer i optimizes its own BESS operation to minimize its *energy not served* (ENS) during the outage period. The local optimization problem for an outage interval is formulated as:

$$\min \sum_{t} \left(P_{i,t}^{\text{load}} - p_{i,t}^{d} \right) \tag{13}$$

where $P_{i,t}^{\text{load}}$ represents the forecasted load of customer i.The battery operation is subject to the same set of physical and operational constraints defined in (5)–(7), which include SoC dynamics. For charging, a similar concept to (4) is applied individually at each customer, such that the charging power does not exceed the available generation at that customer site. Charging is therefore possible only for customers who have both generation and BESS installed.

III. Demonstration

The capability of the proposed framework is demonstrated in the ERCOT system using data from winter storm Uri in 2021 [9]. Two outage management schemes outlined in the previous section are implemented, and their performance is quantified using relevant metrics.

A. Simulation Setup

To demonstrate the proposed framework, a use case is designed to emulate winter storm Uri in February 2021. This use case emulates the distribution grid response for the north weather zone (WZ) of Texas during the storm. The north zone is one of the eight weather zones of ERCOT [10] and experienced a heavy increase in demand during the winter storm. This WZ was modeled using a distribution substation connected to one rural prototypical feeder (R4-25.00-1) [11]. The load is composed of single-family residences, with some light commercial customers, configured with an NZ-specific customer mix and end-user loads (based on EIA data). Further details on the scaling factor, weather data, and calibration are presented in [9]. The simulation spans 10 days in February, with a scarcity event applied from February 15 through February 17, totaling 48 hours. During this period, the system experiences scarcity, and availability reduces to 620 kW.

B. Results

Fig. 2 presents the grid response for the Base (no outage), AMI-RO, and UR cases. In the base case, all loads remain connected, and temperature-dependent loads operate according to user-defined setpoints. This represents the total demand

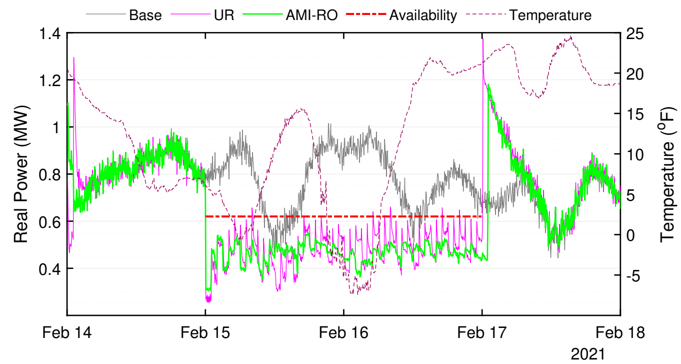

Fig. 2. Grid response for base case and outage management strategies.

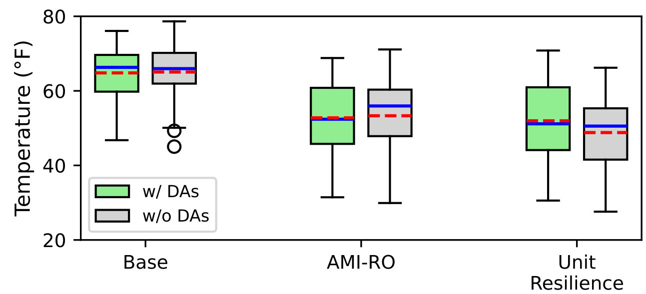

Fig. 3. Average indoor temperature distributions for customers with and without DAs (median: blue solid; mean: red dashed)

without scarcity constraints. From February 15 to February 17, unusually low ambient temperatures increased system demand while derating available generation, resulting in a period of supply scarcity. During scarcity conditions, the outage mechanisms activate and utilize DAs and switching schemes to manage the outage. In both AMI-RO and UR mechanisms, the communicated availability is respected, and the total substation power flow stays within the specified limit as shown in Fig. 2. However, as discussed earlier, the two mechanisms differ in how they manage scarcity and leverage DA's flexibility. In the following subsection, we assess customer-centric metrics and DA scheduling to further analyze and compare the performance of these approaches.

Fig. 3 compares the distribution of average indoor temperatures across the three cases. For each strategy, two customer groups are shown: those equipped with either on-site generation or BESS, and those without any DAs. The overall average indoor temperature is 64.9°F for the Base case, 53.8°F for the AMI-RO case, and 50.7°F for the Unit-Level Resilience (UR) case. The AMI-RO strategy yields an average indoor temperature that is approximately 6.1% higher than the Unit-Level Resilience case. It indicates improved systemwide resilience when customer assets are centrally coordinated. The figure also highlights that the benefits of shared resilience are much more evenly distributed under the AMI-RO strategy. In this case, the average indoor temperatures of customers with DAs (54.0°F) and those without DAs (53.3°F) differ by only 0.7°F. This reflects the fair allocation of DA power under RO. In contrast, under the UR case, customers with DAs maintain an average temperature of 52.0°F, while those without DAs

979-8-3315-8138-1

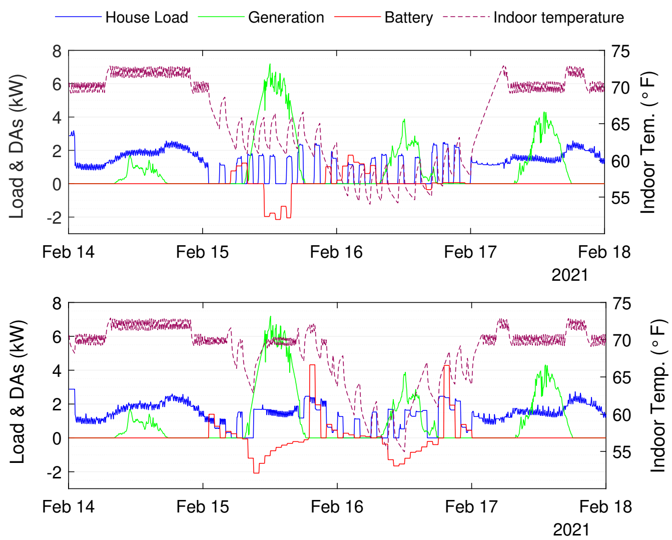

Fig. 4. Comparison of the dispatch strategy of DAs and indoor temperature between AMI-RO (upper) and UR (lower) for a single house.

fall to 48.8°F, representing a difference of more than 3°F between the groups. This larger disparity underscores that, without coordinated control, resilience outcomes depend more heavily on asset ownership.

Fig. 4 illustrates how, without coordinated control, DAs primarily benefit their owners. This figure provides a detailed comparison of how DAs are utilized under the AMI-RO and UR strategies. It shows the house load, on-site generation, battery dispatch, and indoor temperature for a single example home equipped with both generation and BESS. The upper subplot corresponds to the AMI-RO case, and the lower subplot corresponds to the UR case. Under the AMI-RO strategy (upper subplot), during the outage period (Feb. 15-17), the house load (solid blue line) cycles on and off intermittently. The indoor temperature (deep magenta dashed line) rises whenever power is allocated to the home and declines during periods without supply. Negative power values indicate battery charging. During the daytime hours, the battery (solid red line) charges using available on-site generation, and its stored energy is used during nighttime for the community. In contrast, the UR case (lower subplot) shows a notably different dispatch pattern. Here, the battery charges to its maximum whenever on-site generation is available and discharges aggressively when grid power is not allocated. The on-site generation was directly used for the house load as well. As a result, the home maintains a significantly higher indoor temperature compared to the AMI-RO case. On February 15, the indoor temperature remains close to 70°F, whereas under AMI-RO, it stays between 60°F and 65°F because power from DAs is shared across the community rather than being served to individual homes. The difference is also evident in the house load profile. In the UR case, the house load remains fully powered with high local generation during daytime, as the priority is given to the home's own resilience. On Feb. 16, the indoor temperature drops sharply during the early morning hours after the battery is fully exhausted and before any on-site generation is available. During this interval, the home must rely on grid allocations, which occur intermittently. Once on-site generation resumes during the day, the battery recharges and the indoor temperature rises accordingly. Overall, the UR case maintains a higher indoor temperature than the AMI-RO case because the customer's assets are used exclusively for that customer. In contrast, the AMI-RO distributes flexibility from the DAs across the community to improve systemwide resilience.

IV. Conclusions

This paper presents a two-stage outage management framework that coordinates the scheduling of DAs and switching decisions to enhance shared resilience during periods of supply scarcity. Under conditions modeled on the 2021 winter storm, the results show that centrally orchestrated DAs reduce outage durations and maintain higher indoor temperatures for a larger portion of customers compared to unit-level operation, where DA benefits remain confined to their owners. By demonstrating how flexibility from assets can be leveraged collectively rather than individually, the proposed approach provides a practical pathway for DSOs to manage scarcity more effectively and support broader resilience during extreme events, thereby motivating future work on operational practices and incentive structures that enable shared resilience at scale.

References

[1] U.S. Environmental Protection Agency, "Climate change impacts on energy," https://www.epa.gov/climateimpacts/climate-change-impacts-energy, 2025, accessed November 6, 2025.

[2] P. Staff, "Texas and california built different power grids, but neither stood up to extreme weather," *Politico*, February 2021, accessed November 6, 2025. [Online]. Available: https://www.politico.com/news/2021/02/21/texas-california-climate-change-power-grids-470434

[3] S. Poudel, M. G. Yu, M. Mukherjee, S. Hanif, T. D. Hardy, and H. M. Reeve, "A framework to design consumer-centric operational strategies for resilience enhancement," *IEEE Transactions on Industry Applications*, vol. 60, no. 2, pp. 2332–2343, 2024.

[4] Environment America, Clean Energy, Oct 10, 2023. Vermont utility proposes to install battery storage in most homes. [online] Available: https://environmentamerica.org/updates/vermont-utility-proposes-to-install-battery-storage-in-most-homes/.

[5] Northwest Power and Conservation Council, "Behind-the-Meter Solar-Battery Systems: Potential for Load Modification in the Northwest," Accessed: 2025-11-06, Northwest Power and Conservation Council, Tech. Rep., 2021, https://www.nwcouncil.org/2021powerplan_behind-meter-solar-battery/.

[6] J. Einolander, A. Kiviaho, and R. Lahdelma, "Valuing the household power outage self-sustainment capabilities of bidirectional electric vehicle charging," *Applied Energy*, vol. 374, p. 124071, 2024.

[7] M. Mukherjee, M. Maharjan, and T. Hardy, "Transactive emergency power allocation," in *2023 IEEE Power & Energy Society General Meeting (PESGM)*, 2023, pp. 1–5.

[8] A. Breidenbaugh, CPower, "Everything you need to know about new york's new der aggregation participation model," https://cpowerenergy.com/everything-you-need-to-know-about-new-yorks-new-der-aggregation-participation-model, 2024, online Accessed: November, 2025.

[9] S. Hanif, M. Mukherjee, S. Poudel, M. G. Yu, R. A. Jinsiwale, T. D. Hardy, and H. M. Reeve, "Analyzing at-scale distribution grid response to extreme temperatures," *Applied Energy*, vol. 337, p. 120886, 2023.

[10] Electric Reliability Council of Texa, "Ercot weather zone map." [Online]. Available: https://www.ercot.com/news/mediakit/maps

[11] K. P. Schneider, Y. Chen, D. P. Chassin, R. G. Pratt, D. W. Engel, and S. E. Thompson, "Modern grid initiative distribution taxonomy final report," Pacific Northwest National Laboratory, Tech. Rep., 11 2008. [Online]. Available: https://www.osti.gov/biblio/1040684